Supporting Information

Modulation of interfacial electronic structure in Ni_3P/NiFe LDH p-n junction for efficient oxygen evolution at ampere-level current density

Xiaochen Zhang,[a] Hui Xue,[*a] Jing Sun,[a] Niankun Guo,[a] Tianshan Song,[a] Jiawen Sun,[a] Yi-Ru Hao,[a] and Qin Wang[*a]

[a] College of Chemistry and Chemical Engineering, Inner Mongolia University, Hohhot, 010021 (P. R. China)

*Corresponding authors: E-mail: qinwang@imu.edu.cn (Q. Wang)

Material characterization

Morphology and structure Characterization: XRD patterns of the samples were measured on a powder X-ray diffraction system (XRD, PuXi XD3) using Cu Kα radiation (λ = 0.15405 nm). SEM analysis was carried out on the QUANTA FEG 400 thermal field emission scanning electron microanalyzer of FEI company in the United States. The test conditions: accelerated voltage of 20000 V. Transmission electron microscope (TEM) and high-resolution transmission electron microscope (HRTEM) images were recorded on Japan-JEOL-JEM 2100F transmission electron microscope system. The X-ray photoelectron spectrometer used in this paper is VG Scientific ESCALAB Mark II. The test conditions: excitation source Al Kα ray source, power of about 300 W, and basic vacuum of 3×10^{-9} mbar. All the measured elemental data are corrected by the C 1s peak at 284.8 eV. The d-band center was obtained by using the ultraviolet photoelectron spectrometer, the model was ESCALAB Xi+, and the test conditions: ultraviolet light source He I, vacuum degree 10^{-8} mbar. Diffuse reflection absorption curve is obtained by using UV-VIS spectrometer (UH4150), and the test band is 200-2500 nm.

Electrochemical measurement

Electrodeposition preparation of samples and all electrochemical performance tests were carried out on Brilliance Electrochemical Workstation (CHI 760E, CH Instruments, Shanghai). Electrolyte is 1 M KOH, and a simulated seawater test is conducted using a solution of 1 M KOH and 0.5 NaCl.

HER and OER tests involved in this paper were all carried out in a three-electrode

system, with carbon rod as the counter electrode, Hg/HgO as the reference electrode, and the synthesized catalyst as the working electrode (the test area is 0.5×0.5 cm^2). The electrochemical total hydrolysis reaction adopts a double-electrode system, in which the cathode and anode are self-supporting electrodes synthesized in the experiment.

All voltages mentioned in this paper have been calibrated to the voltage of a relatively reversible hydrogen electrode (RHE). The measured voltage (relative to the Hg/HgO electrode) was calibrated to the RHE voltage by the Nernst equation:

$$E_{RHE} = E_{Hg/HgO} + 0.059 \times pH + 0.098$$

In the experiment, all LSV polarization curves were measured at a scanning rate of 2 $mV \cdot s^{-1}$, and 85% manual iR compensation was carried out in the test. Before LSV test, the samples were tested by cyclic voltammetry (CV) at fast scanning speed to keep the electrode surface basically stable. For OER, the voltage window is set to 0 - 1 V, and for HER reaction, the voltage window is set to -1.5 - -0.8 V. For the OER process, in order to avoid the overlapping of the oxidation peak and the OER signal, negative scanning (inverse scanning) was chosen to obtain the experimental data. When electrochemical impedance spectroscopy (EIS) is tested, the frequency range is set to 10^{-1} to 10^6 Hz and the amplitude is 5 $mV \cdot s^{-1}$, and the same group of samples are tested at the same voltage. In order to obtain the C_{dl} of catalytic materials, we measured the CV curves at different scanning rates (10, 20, 30, 40, 50, 60 $mV \cdot s^{-1}$) in the non-Faraday voltage range, drew the curve between the corresponding scanning rate and the current difference at the midpoint of the potential range and fitted it, and

selected the voltage range of oxygen evolution reaction as 0 - 0.1 V; For the hydrogen evolution reaction, the voltage range is -0.874 - -0.774 V. The electric double layer capacitance is proportional to the electrochemical active surface area, and according to this relationship, the electrochemical active surface area of catalysts can be obtained. The stability of the catalyst was characterized by chronoamperometry (i-t) and chronopotentiometry (v-t).

Calculation of TOF

The current density map of OER can be transformed into turnover frequency (TOF) map using the formula: TOF = j*A/ (4* F*n), where: j is the current density ($A \cdot cm^{-2}$), A is the active surface area of each electrode, 4 represents the four-electron transfer process, F is the Faraday constant (96485.3 $C \cdot mol^{-1}$), and n is the number of active site moles.

Calculate the Faraday efficiency

Faraday efficiency (FE) is calculated by the drainage gas collection method, and the formula is $FE=n_{gas}*Z*F/(I*t)$. Where Z is the number of electrons needed to form A molecule of gas product (O_2 is 4, H_2 is 2), F is Faraday's constant (96485.3 $C \cdot mol^{-1}$), I is current (A), and t is time (s).

DFT calculations

We have employed the first-principles to perform spin-polarization density functional theory (DFT) calculations within the generalized gradient approximation (GGA) using the Perdew-Burke-Ernzerhof (PBE) formulation.[1-3] We have chosen the projected augmented wave (PAW) potentials to describe the ionic cores and take valence electrons into account using a plane wave basis set with a kinetic energy cutoff of 520 eV.[4,5] Partial occupancies of the Kohn-Sham orbitals were allowed using the Gaussian smearing method and a width of 0.05 eV. The electronic energy was considered self-consistent when the energy change was smaller than 10−5 eV. A geometry optimization was considered convergent when the energy change was smaller than 0.05 eV $Å^{-1}$. The vacuum spacing in a direction perpendicular to the plane of the structure is 18 Å. The Brillouin zone integration is performed using 2×2×1 Monkhorst-Pack k-point sampling for a structure. Finally, the adsorption energies (Eads) were calculated as Eads= Ead/sub -Ead -Esub, where Ead/sub, Ead, and Esub are the total energies of the optimized adsorbate/substrate system, the adsorbate in the structure, and the clean substrate, respectively. The free energy was calculated using the equation:

G=Eads+ZPE-TS

where G, Eads, ZPE and TS are the free energy, total energy from DFT calculations, zero point energy and entropic contributions, respectively.

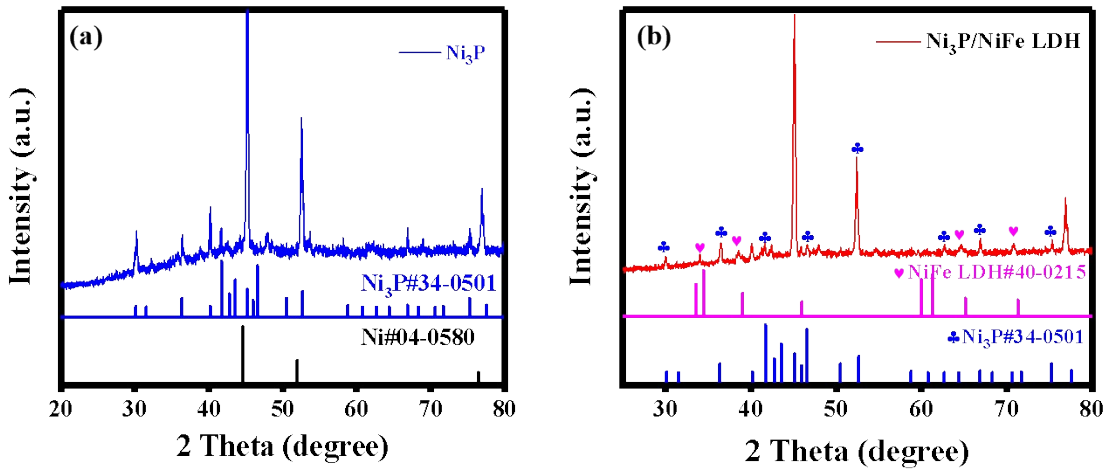

Fig. S1 XRD patterns of (a) Ni_3P; (b) Ni_3P/NiFe LDH.

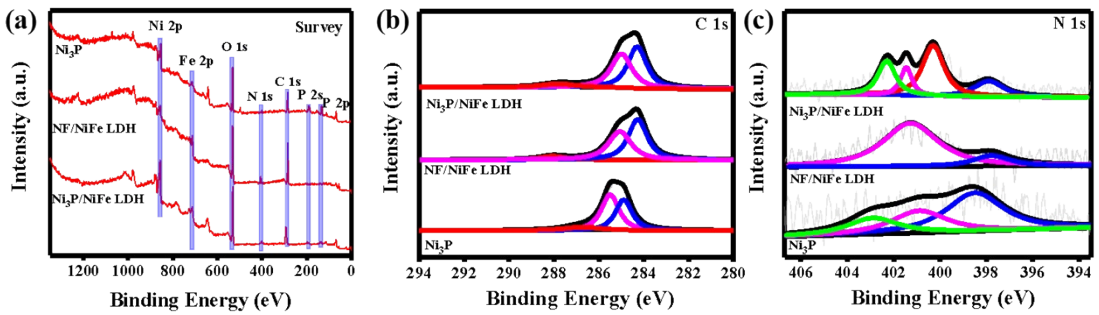

Fig. S2 XPS spectra of Ni_3P, NF/NiFe LDH, and Ni_3P/NiFe LDH. (a) XPS survey; (b) C 1s; (c) N 1s.

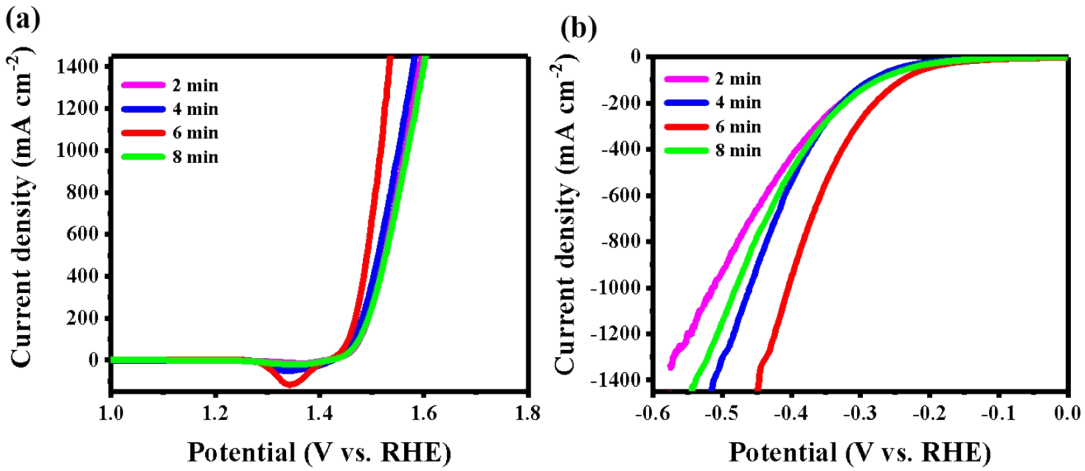

Fig. S3 Adjusting the electrodeposition time: (a) OER LSV polarization curves; (b) HER LSV polarization curves.

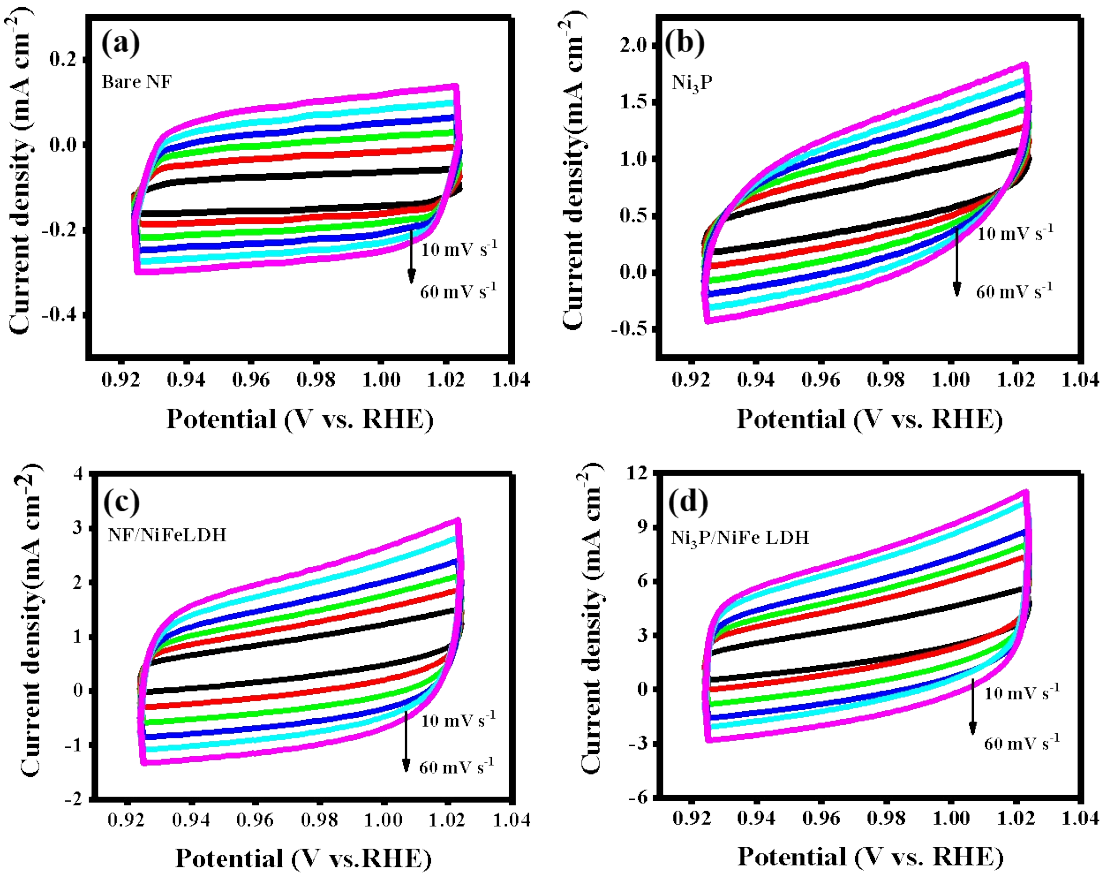

Fig. S4 OER CV curves of (a) Bare NF, (b) Ni_3P, (c) NF/NiFe LDH, (d) Ni_3P/NiFe LDH catalysts at different scan rates of 10, 20, 30, 40, 50, and 60 $mV \cdot s^{-1}$ in a non-Faradaic region.

The specific capacitance of the flat reference material of 1 cm^2 is usually 40 $\mu F \cdot cm^{-2}$, and the electrochemically active surface area of the catalyst is calculated by analogy.

Calculation of ECSA for each catalyst:

$ECSA = C_{dl}/C_s$

ECSA Bare NF = 2.8 $mF \cdot cm^{-2}$/40 $\mu F \cdot cm^{-2}$ = 70 cm^{-2}_{ECSA}

ECSA Ni_xP_y = 10.4 $mF \cdot cm^{-2}$/40 $\mu F \cdot cm^{-2}$ = 260 cm^{-2}_{ECSA}

ECSA NF/NiFe LDH = 24.8 $mF \cdot cm^{-2}$/40 $\mu F \cdot cm^{-2}$ = 620 cm^{-2}_{ECSA}

ECSA Ni_xP_y/NiFe LDH = 44.8 $mF \cdot cm^{-2}$/40 $\mu F \cdot cm^{-2}$ = 1120 cm^{-2}_{ECSA}

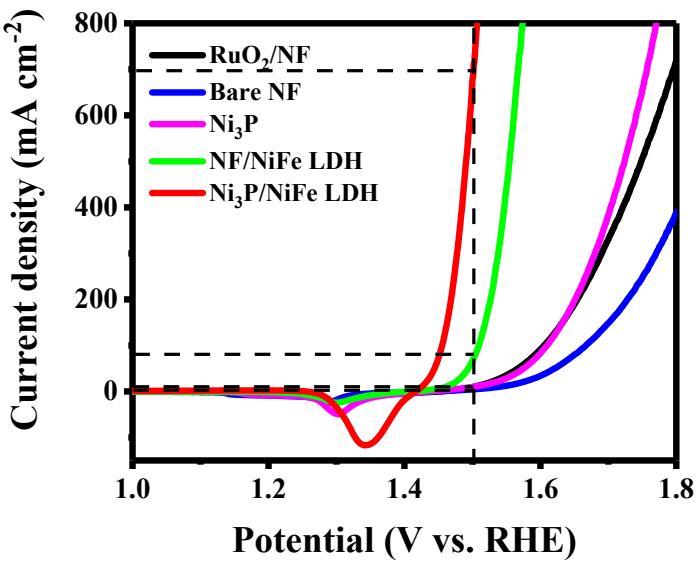

Fig. S5 OER polarization curves of catalysts in 1 M KOH.

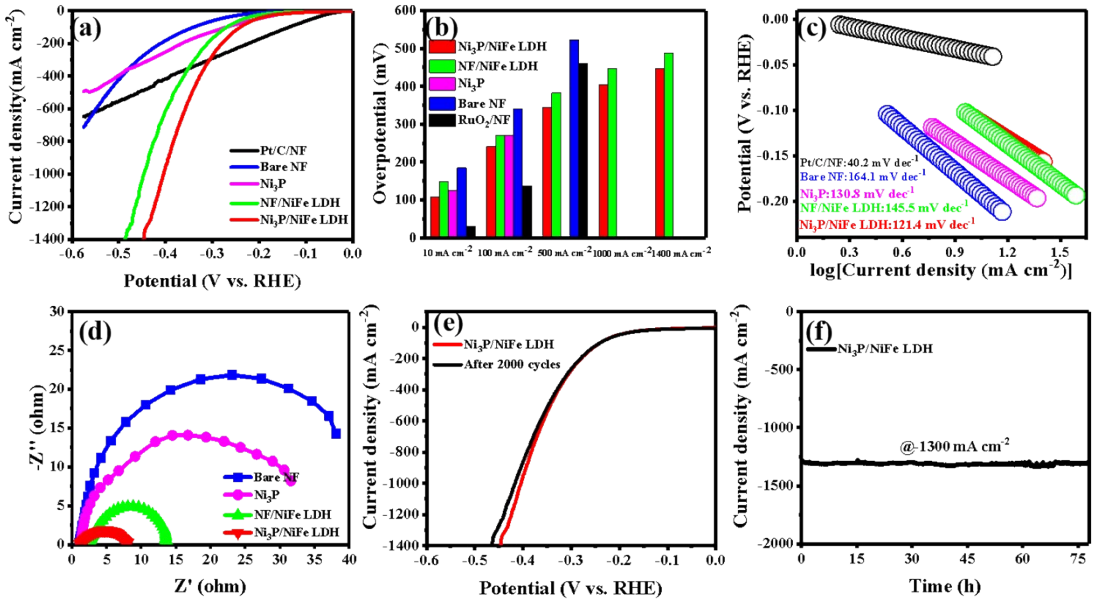

Fig. S6 (a) HER polarization curves of bare NF, Ni_3P, NF/NiFe LDH, and Ni_3P/NiFe LDH in 1.0 M KOH solution; (b) HER overpotentials at current densities; (c) Tafel slopes; (d) EIS; (e) LSV curves of Ni_3P/NiFe LDH before and after 2000 CV cycles; (f) Timing current (i-t) stability test.

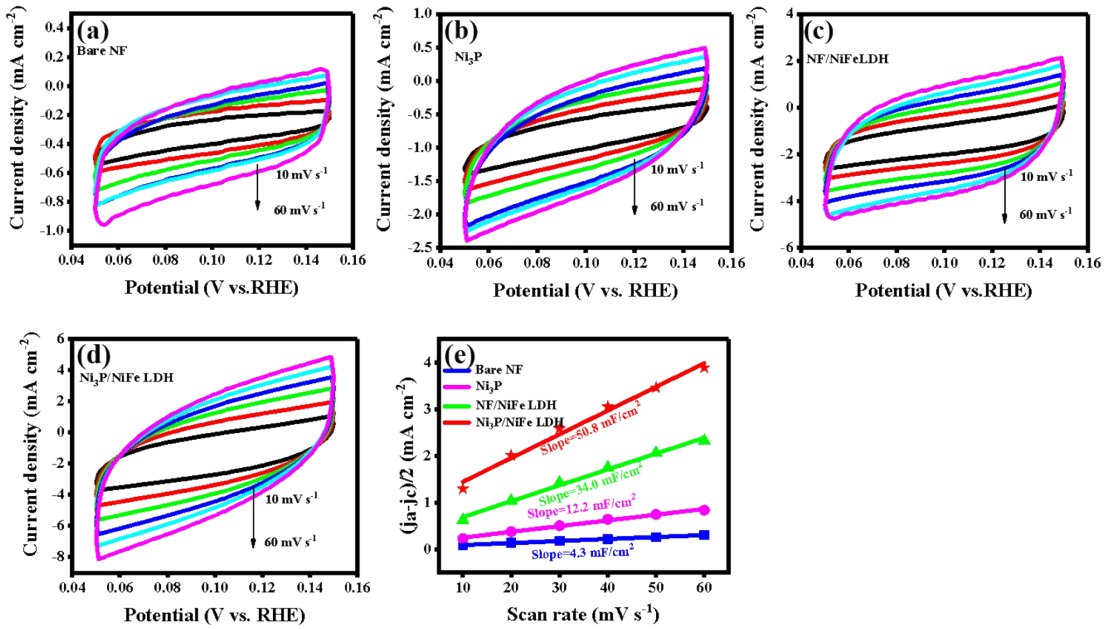

Fig. S7 (a-d) HER CV curves of bare NF, Ni_3P, NF/NiFe LDH, and Ni_3P/NiFe LDH at different scanning rates (10, 20, 30, 40, 50, and 60 $mV \cdot s^{-1}$) in the non-Faraday region; (e) C_{dl}.

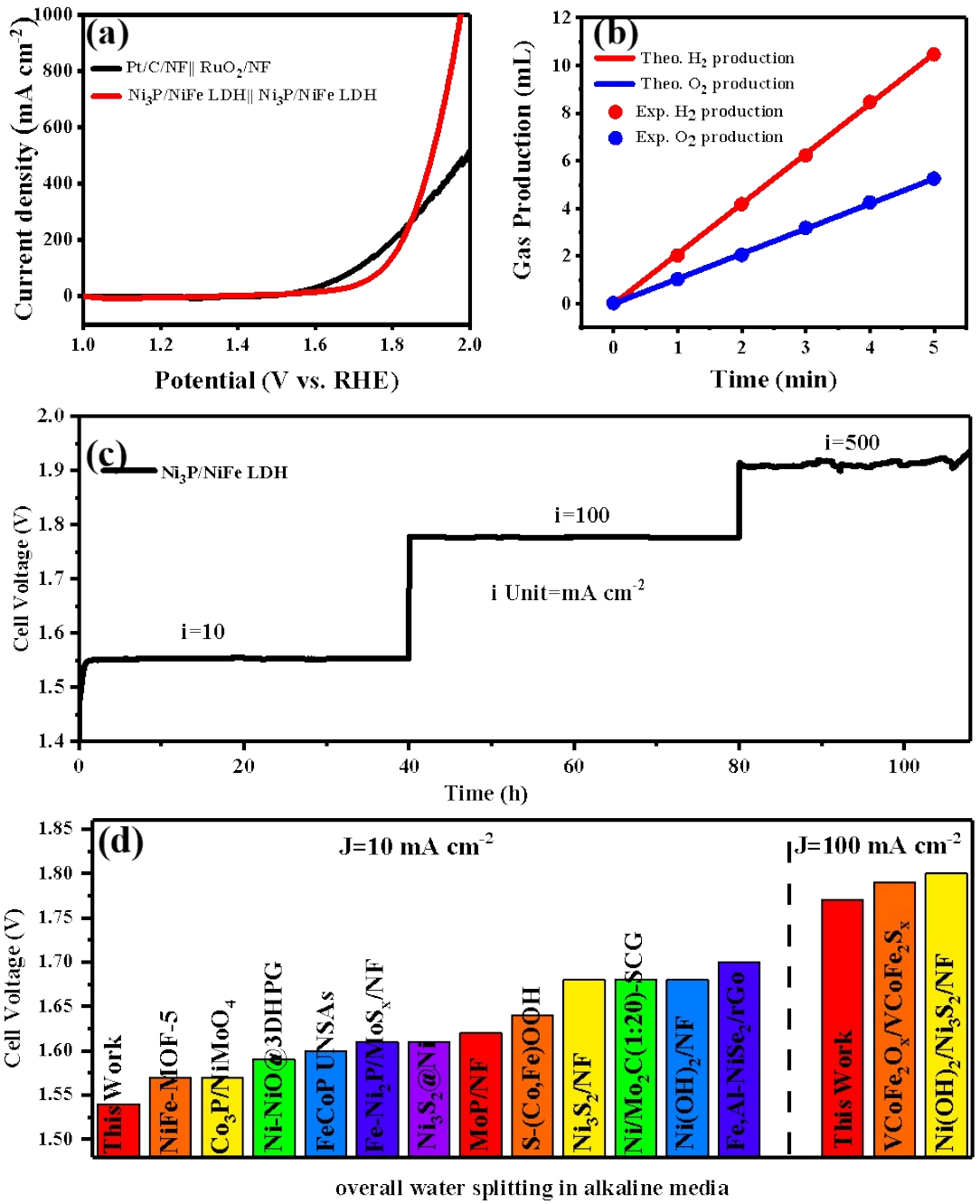

Fig. S8 (a) LSV polarization curve of Ni_3P/NiFe LDH||Ni_3P/NiFe LDH and RuO_2/NF||Pt/C/NF double electrode system in 1.0 M KOH solution; (b) Faraday efficiency; (c) Continuous constant potential (v-t) stability test; (d) Comparison of overall water splitting properties at 10 and 100 mA·cm^{-2}.

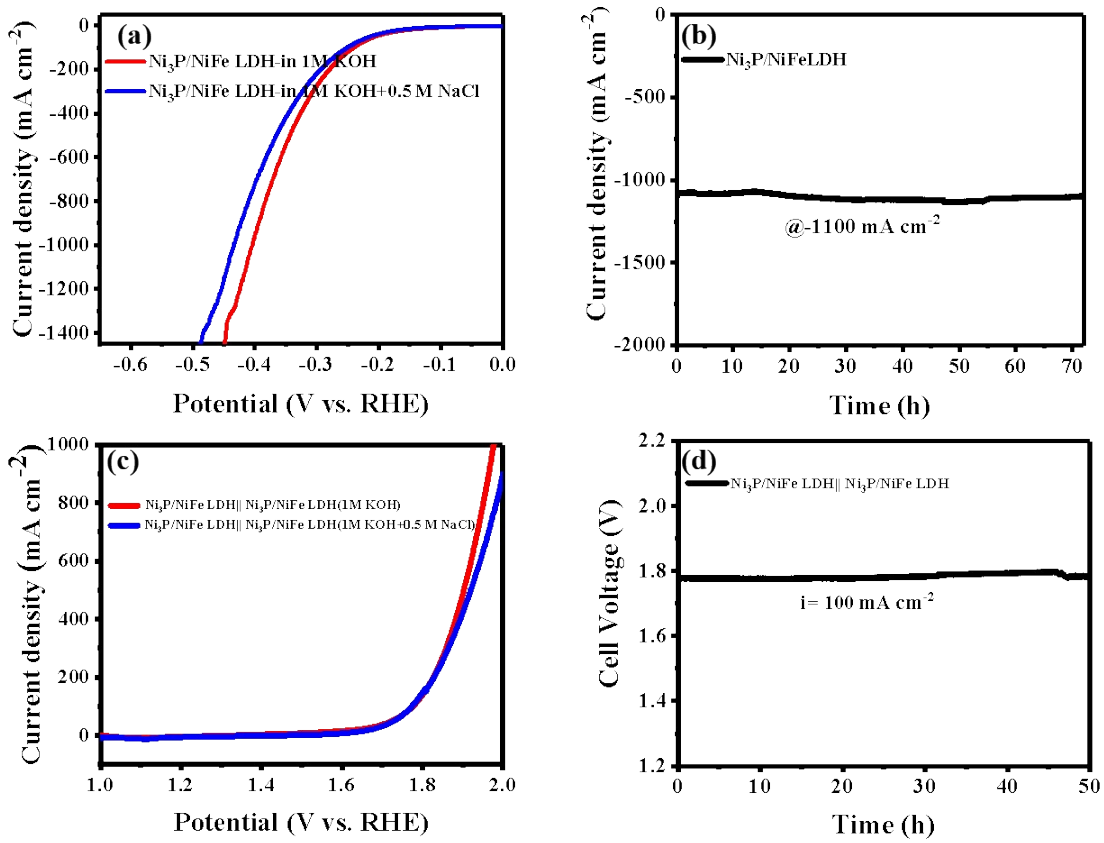

Fig. S9 Ni_3P/NiFe LDH in 1 M KOH and simulated seawater electrolyte (1 M KOH + 0.5 M NaCl). (a) HER LSV curves; (b) Timing current (i-t) stability test in a simulated seawater electrolyte; (c) totally dissolved (seawater) water test of Ni_3P/NiFe LDH||Ni_3P/NiFe LDH double electrode system; (d) stability test in a simulated seawater electrolyte.

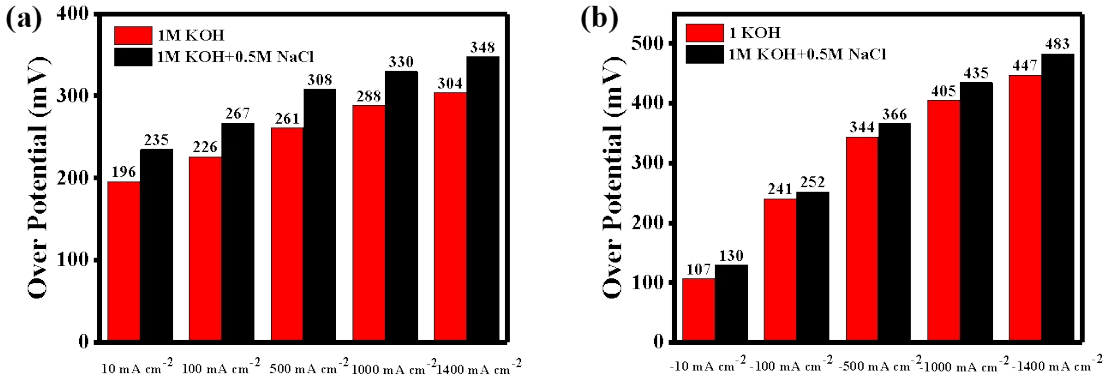

Fig. S10 (a) OER overpotentials required for j = 10, 100, 500, 1000, and 1400 mA·cm^{-2}. (b) HER overpotentials required for j = -10, -100, - 500, -1000, and -1400 mA·cm^{-2}.

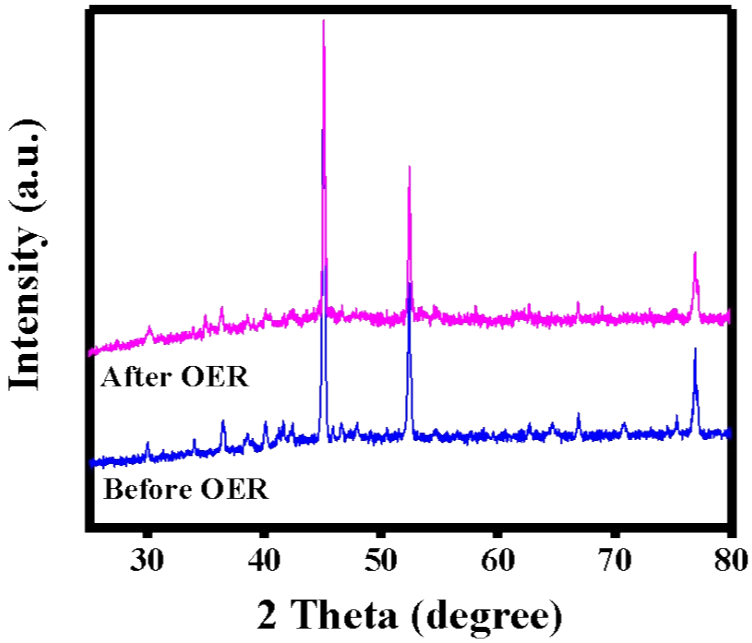

Fig. S11 XRD pattern of Ni_3P/NiFe LDH before and after reaction.

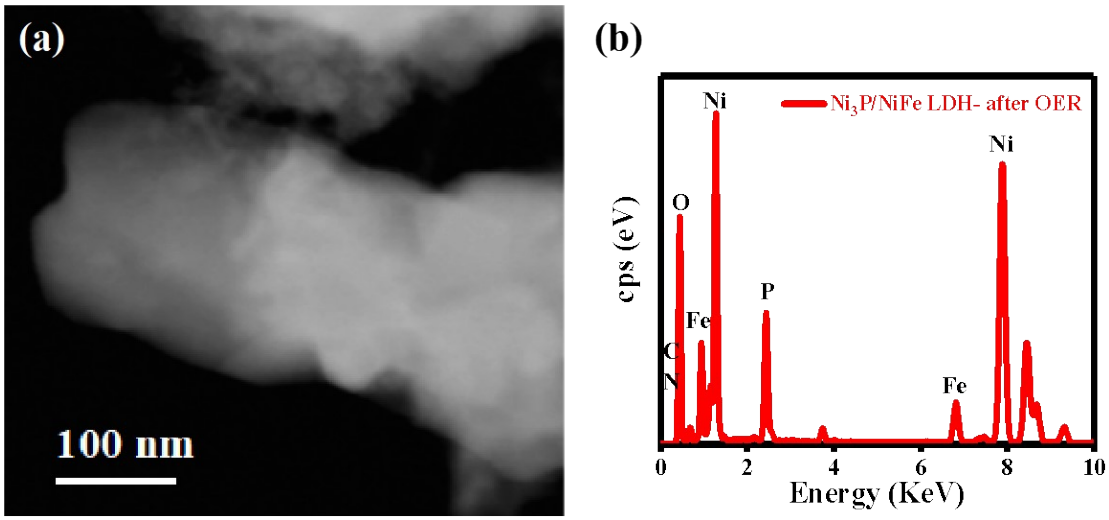

Fig. S12 (a) HAADF-STEM image; (b) STEM-EDX spectra of Ni_3P/NiFe LDH after OER.

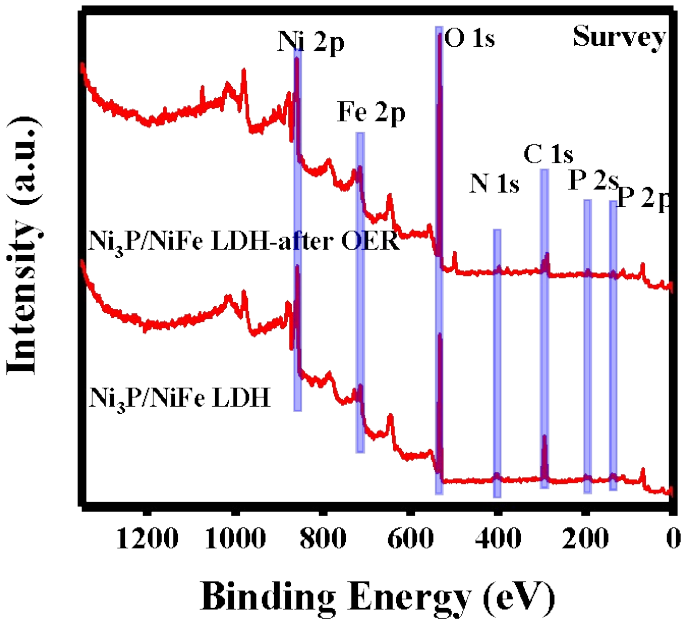

Fig. S13 XPS survey of Ni_3P/NiFe LDH before and after reaction.

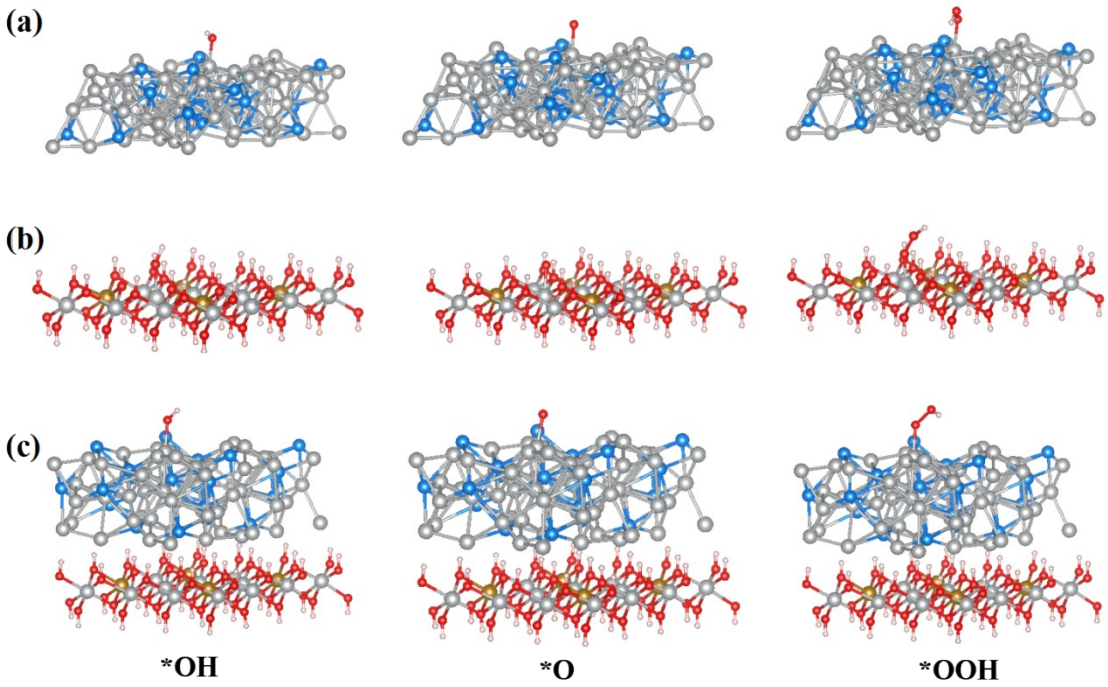

Fig. 14 Intermediate state (*OOH, *O, *OH) structure of OER process (a) Ni_3P; (b) NiFe LDH; (c) Ni_3P/NiFe LDH.

Table S1. XPS elemental quantitative analysis results of Ni_3P, NF/NiFe LDH, and Ni_3P/NiFe LDH.

atomic ratio / sample	Ni	Fe	P	O	C	N
Ni_3P	**11.77**		**19.79**	**32.87**	**32.75**	**2.82**
NF/NiFe LDH	**9.01**	**10.08**		**36.28**	**38.67**	**5.96**
Ni_3P/NiFe LDH	**9.96**	**9.18**	**8.88**	**31.02**	**33.27**	**7.69**

Table S2. Comparison of OER catalytic activity between Ni_3P/NiFe LDH and recently reported advanced electrocatalyst in 1 M KOH solution at current density of 10 $mA \cdot cm^{-2}$.

Catalyst	η_{10}* (mV)	Tafel slope (mV dec^{-1})	Reference
Ni_3P/NiFe LDH	**196**	**25.2**	**This work**
NF@Fe_2-Ni_2P/C	205	52	*ACS Catal.* **2019,** *9* (10), 8882-8892.
NiFe LDH-NS@DG10	210	52	*Adv. Mater.* **2017,** *29* (17), 1700017.
Ni_2P-Ni_3S_2 HNAs/NF	210	62	*Nano Energy.* **2018,** *51*, 26-36.
Gd-NiFe-LDH@CC	210	40.9	*J. Mater. Chem. A.* **2021,** *9* (5), 2999-3006.
NiFe-MOF	215	49.1	*Adv. Funct. Mater.* **2021,** *31* (33), 2102066.
Ru/Ni_3V-LDH	225	33	*J. Am. Chem. Soc.* **2022,** *144* (3), 1174-1186.
Ni/CeO_2@N-CNFs	230	54.2	*Small.* **2022,** *18* (13), 2106592.
$NiPS_{2.7}Se_{0.3}$	250	76	*Adv. Funct. Mater.* **2021,** *31* (19), 2100618.
CoFe LDHs-Ar/NF	266	37.85	*Angew. Chem. Int. Ed.* **2017,** *56* (21), 5867-5871.
$NiCo_2S_4$@NiFe LDH	370	96	*App. Catal. B-Environ.* **2021,** *286*, 119869.

Table S3. Comparison of OER catalytic activity between Ni_3P/NiFe LDH and recently reported advanced electrocatalyst in 1 M KOH solution at current density of 100 $mA \cdot cm^{-2}$.

Catalyst	η_{100}* (mV)	Tafel slope (mV dec^{-1})	Reference
Ni_3P/NiFe LDH	**226**	**25.2**	**This work**
NiFc MOF/NF	240	44.1	*Angew. Chem. Int. Ed.* **2021,** *60* (23), 12770-12774.
FeNi-LDH/CoP/CC	248.9	33.5	*Angew. Chem. Int. Ed.* **2019,** *58* (34), 11903-11909.
NiFeRu LDH	258	-	*Adv. Mater.* **2018,** *30* (10), 1706279.
Ni-Fe NPs	270	58	*Nat. Commun.* **2019,** *10* (1), 5599.
NiMoN@NiFeN	277	58.6	*Nat. Commun.* **2019,** *10* (1), 5106.
S,P-(Ni,Mo,Fe)OOH/NiMoP/Wood aerogel	279	56.7	*Appl. Catal. B-Environ.* **2021,** *293*, 120215.
CoFeZr oxides	290	54.2	*Adv. Mater.* **2019,** *31* (28), 1901439.
Strained FeP_2/NF	315	56	*Adv. Funct. Mater.* **2020,** *30* (12), 1907791.
Cu@CoFe LDH	318	44.4	*Nano Energy.* **2017,** *41*, 327-336.
FeCoNi nanotube array	390	49.9	*Nano Res.* **2016,** *9* (3), 831-836.

Table S4. Comparison of OER catalytic activity between Ni_3P/NiFe LDH and recently reported advanced electrocatalyst in 1 M KOH solution at current density of 500 $mA \cdot cm^{-2}$.

Catalyst	η_{500}* (mV)	Tafel slope (mV dec^{-1})	Reference
Ni_3P/NiFe LDH	**261**	**25.2**	**This work**
$Fe_{0.01}$&Mo-NiO	272	51.1	*Energy & Environ. Sci.* **2022,** *15* (9), 3945-3957.
$NiMo_x$/NiMoS	278	34	*Nat. Commun.* **2020,** *11* (1), 5462.
NiFe-MOF	297	49.1	*Adv. Funct. Mater.* **2021,** *31* (33), 2102066.
Cu@NiFe LDH	311	27.8	*Energy & Environ. Sci.* **2017,** *10* (8), 1820-1827.
NiMoN@NiFeN	337	58.6	*Nat. Commun.* **2019,** *10* (1), 5106.
CoP_x@FeOOH	337	37.6	*Appl. Catal. B-Environ.* **2021,** *294*, 120256.
Co_9S_8@Fe_3O_4	350	54	*ACS Catal.* **2022,** *12* (8), 4318-4326.
Ni-Fe-OH@Ni_3S_2/NF	370	-	*Adv. Mater.* **2017,** *29* (22), 1700404.
Ni-Mo-B HF	407	79.0	*Adv. Funct. Mater.* **2022,** *32* (4), 2107308.

Table S5. Comparison of OER catalytic activity between Ni_3P/NiFe LDH and recently reported advanced electrocatalyst in 1 M KOH solution at current density of 1000 mA·cm^{-2}.

Catalyst	η_{1000}* (mV)	Tafel slope (mV dec^{-1})	Reference
Ni_3P/NiFe LDH	**288**	**25.2**	**This work**
NF@Fe_2-Ni_2P/C	300	52	*ACS Catal.* **2019,** *9* (10), 8882-8892.
$FeNiCoCrMnS_2$	308	39.1	*Adv. Funct. Mater.* **2021,** *31* (48), 2106229.
Cu@NiFe LDH	315	27.8	*Energy & Environ. Sci.* **2017,** *10* (8), 1820-1827.
NiFe LDH/NiS	325	60.1	*Adv. Energy Mater.* **2021,** *11* (46), 2102353.
Zn-(Ni/FeOOH)@NF	330	33	*Small.* **2022,** *18* (37), 2203710.
CoS@NiFe/NF	330	73.1	*Chem. Asian. J.* **2020,** *15* (9), 1484-1492.
$NiFe(OH)_x$/FeS/1F	332	-	*Adv. Funct. Mater.* **2019,** *29* (36), 1902180.
Ni_2P-Fe_2P/NF	337	58	*Adv. Funct. Mater.* **2021,** *31* (1), 2006484.
0.05-$MnCuCo_2Se$	345	68	*Appl. Catal. B-Environ.* **2022,** *316*, 121649.
Fe-CoP/NF	428	36	*Adv. Sci.* **2018,** *5* (10), 1800949.

Table S6. Comparison of water splitting activity between Ni_3P/NiFe LDH and other reported electrocatalysts in 1 M KOH solution at current density of 10 $mA \cdot cm^{-2}$.

Catalyst	voltage @j_{10} (V)	Durability	Substrate	Reference
Ni_3P/NiFe LDH	**1.54**	**108 h**	**NF**	**This work**
NiFe-MOF-5	1.57	24 h	NF	*Inorg. Chem. Front.,* ***2021,*** *8 (11), 2889-2899.*
$Co_3P/NiMoO_4$	1.57	12 h	NF	*Ceram. Int.,* ***2019,*** *45 (14), 17128-17136.*
Ni-NiO@3DHPG	1.59	-	SCG	*Electro. Acta,* ***2019,*** *298, 163-171.*
FeCoP UNSAs	1.6	20 h	NF	*Nano Energy,* ***2017,*** *41, 583-590.*
Fe-Ni_2P/MoS_x/NF	1.61	36 h	NF	*Adv. Mater.,****2020,*** *7 (12), 1901926.*
Ni_3S_2@Ni	1.61	30 h	NF	*J. Energy Chem.,* ***2020,*** *46, 178-186.*
MoP/NF	1.62	20 h	NF	*Small,* ***2018,*** *2 (5), 1700369.*
S-(Co,Fe)OOH	1.64	50 h	Fe foam	*Nanoscale, Adv.,* ***2021,*** *3 (22), 6386-6394.*
Ni_3S_2/NF	1.68	14 h	NF	*Nanoscale,* ***2018,*** *10 (36), 17347-17353.*
Ni/Mo_2C (1:20)-SCG	1.68	27 h	SCG	*Inter. J. Hydrogen Energy,* ***2022,*** *47 (2), 761-771.*
$Ni(OH)_2$/ NF	1.68	24 h	NF	*ACS Appl. Mater. & Inter.,* ***2016,*** *8 (49), 33601-33607.*
Fe, Al-$NiSe_2$/rGo	1.7	80000 s	rGO	*Nanoscale,* ***2020,*** *12 (25),*

13680-13687.

Table S7. Comparison of water splitting activity between Ni_3P/NiFe LDH and other reported electrocatalysts in 1 M KOH solution at current density of 100 $mA \cdot cm^{-2}$.

Catalyst	voltage@ j_{100} (V)	Durability	Substrate	Reference
Ni_3P/NiFe LDH	**1.77**	**108 h**	**NF**	**This work**
$VCoFe_2O_x/VCoFe_2S_x$	1.79	-	NF	*New J. Chem.,* ***2022,*** *46 (8), 3555-3559.*
Fe, Al-$NiSe_2$/rGo	1.8	100 h	NF	*Energy & Fuels,* ***2019,*** *33 (11), 12052-12062.*

Table S8. Comparison of OER catalytic activity between Ni_3P/NiFe LDH and recently reported advanced electrocatalyst in 1 M KOH + 0.5 M NaCl solution at current density of 100 $mA \cdot cm^{-2}$.

Catalyst	η_{100}* (mV)	Durability	Substrate	Reference
Ni_3P/NiFe LDH	**267**	**78 h**	**NF**	**This work**
Gly-@NCP	268	20 h	CP	*Adv. Sci.,* ***2021,*** *8 (14), 2100498.*
S-(Ni,Fe)OOH	278	100 h	NF	*Energy-Environ. Sci.,* ***2020****, 13 (10), 3439-3446.*
NiMoN@NiFeN	286	100 h	NF	*Nat. Commun., 10, 5106 (****2019).***
$(NiFeCoV)S_2$	299	50 h	NF	*J. Colloid Inter. Sci.,* ***2023,*** *645, 724-734.*
CoP_x@FeOOH	300	80 h	NF	*Appl. Catal. B-Environ.,* ***2021,*** *294, 120256.*
Ni_2P-Fe_2P/NF	305	48 h	NF	*Adv. Funct. Mater.,* ***2021,*** *31 (1), 2006484.*
Fe-$Ni(OH)_2$/ Ni_3S_2@NF	320	27 h	NF	*Nano Research,* ***2021,****14, 1149–1155.*
NiFe/NiS_x-Ni	330	500 h	NF	*P. National Acad. Sci.,* ***2019,*** *116 (14), 6624-6629.*
Cr-Co_xP	330	140 h	NF	*Adv. Funct. Mater.,* ***2023,*** *2214081.*
NiCoHPi@Ni_3N/NF	365	120 h	NF	*ACS Appl. Mater. Inter.,* ***2022,*** *14 (19), 22061-22070.*
Co-Fe-O-B-10	434	20 h	GC	*ACS Appl. Energy Mater.,* ***2020,*** *3 (8), 7619-7628.*

Note: NF (Ni foam), CP (Carbon Paper), GC (Glassy Carbon).

Table S9. Comparison of OER catalytic activity between Ni_3P/NiFe LDH and recently reported advanced electrocatalyst in 1 M KOH + 0.5 M NaCl solution at current density of 500 $mA \cdot cm^{-2}$.

Catalyst	η_{1000}* (mV)	Durability	Substrate	Reference
Ni_3P/NiFe LDH	**308**	**78 h**	**NF**	**This work**
CoP_x@FeOOH	360	80 h	NF	*Appl. Catal. B-Environ.,* ***2021****, 294, 120256.*
Cr-Co_xP	375	140 h	NF	*Adv. Funct. Mater.,* ***2023****, 2214081.*
S, B-(CoFeV)OOH	388	50 h	NF	*ACS Appl. Energy Mater.,* ***2021,*** *4 (7), 6942-6956.*
NiCoHPi@Ni_3N/NF	425	120 h	NF	*ACS Appl. Mater.s & Inter.,* ***2022****, 14 (19), 22061-22070.*

Table S10. Comparison of OER catalytic activity between Ni_3P/NiFe LDH and recently reported advanced electrocatalyst in 1 M KOH + 0.5 M NaCl solution at current density of 1000 $mA \cdot cm^{-2}$.

Catalyst	η_{1000}* (mV)	Durability	Substrate	Reference
Ni_3P/NiFe LDH	**330**	**78 h**	**NF**	**This work**
Cr-Co_xP	404	140 h	NF	*Adv. Funct. Mater.*, ***2023***, *2214081.*
Go@Fe@Ni-Co/NF	434	0.2 h	NF	*J. Mater. Chem. A.*, ***2020***, *8 (46), 24501-24514.*

References

1. G. Kresse, J. Furthmüller, Efficiency of Ab-Initio Total Energy Calculations for Metals and Semiconductors Using a Plane-Wave Basis Set. *Comput. Mater. Sci.*, 1996, **6**, 15-50.
2. G. Kresse, J. Furthmüller, Efficient Iterative Schemes for Ab Initio Total-Energy Calculations Using a Plane-Wave Basis Set. *Phys. Rev. B*, 1996, **54**, 11169-11186.
3. J. P. Perdew, K. Burke, M. Ernzerhof, Generalized Gradient Approximation Made Simple. *Phys. Rev. Lett.*, 1996, 77, 3865-3868.
4. G. Kresse, D. Joubert, From Ultrasoft Pseudopotentials to the Projector Augmented-Wave Method. *Phys. Rev. B*, 1999, **59**, 1758-1775.
5. P. E. Blöchl, Projector Augmented-Wave Method. *Phys. Rev. B*, 1994, **50**, 17953-17979.